A THERMO-ELASTO-VISCOPLASTIC MODEL
FOR COMPOSITE MATERIALS
AND ITS FINITE ELEMENT ANALYSIS

Eui Sup Shin[*]
Department of Aerospace Engineering
Chonbuk National University, Chonju 561-756, South Korea

Abstract

A constitutive model on orthotropic thermo-elasto-viscoplasticity for fiber-reinforced composite materials is illustrated, and their thermomechanical responses are predicted with the fully-coupled finite element formulation. The unmixing-mixing scheme can be adopted with the multipartite matrix method as the constitutive model. Basic assumptions based upon the composite micromechanics are postulated, and the strain components of thermal expansion due to temperature change are included in the formulation. Also, more than two sets of mechanical variables, which represent the deformation states of multipartite matrix, can be introduced arbitrarily. In particular, the unmixing-mixing scheme can be used with any well-known isotropic viscoplastic theory of the matrix material. The scheme unnecessitates the complex processes for developing an orthotropic viscoplastic theory.

The governing equations based on fully-coupled thermomechanics are derived with constitutive arrangement by the unmixing-mixing concept. By considering some auxiliary conditions, the initial-boundary value problem is completely set up. As a tool of numerical analyses, the finite element method is used with isoparametric interpolation for the displacement and the temperature fields. The equation of motion and the energy conservation equation are spatially discretized, and then the time marching techniques such as the Newmark method and the Crank-Nicolson technique are applied. To solve the ultimate nonlinear simultaneous equations, a successive iteration algorithm is constructed with subincrementing technique. As a numerical study, a series of analyses are performed with the main focus on the thermomechanical coupling effect in composite materials. The progress of viscoplastic deformation, the stress-strain relation, and the temperature history are carefully examined when composite laminates are subjected to repeated cyclic loading.

Key Words : Unmixing-mixing scheme, Thermo-elasto-viscoplasticity,
Thermomechanical coupling, Numerical analysis

Introduction

Advanced composite materials have successfully been used in severe thermal and/or mechanical environment for various field's applications [1]. Recently, to take an example, the interest in hypersonic vehicles has brought attention to the advanced materials because structural components are operated under extremely severe aerothermal conditions such as aerodynamic heating [2]. Thermoplastic and metal-matrix composites may experience an appreciable amount of viscoplastic deformation, especially at high temperatures.

In general, the inherent anisotropy of composites increases the difficulty in describing the viscoplastic deformation. Up to date, many kinds of constitutive theories have been suggested to simulate the viscoplastic response of the anisotropic materials. Most of the theories were modified and extended from the classical plasticity models or the unified viscoplastic models for materials

* : Assistant Professor

by introducing macroscopic composite mechanics[3-7]. On the other hand, there have been several efforts made, based on micromechanics which predicts the overall behavior of composite from the individual properties of constituent materials [8-11]. Recently, Kim et al. proposed an unmixing-mixing concept and considered general procedure to systematically analyze the viscoplastic behavior of composites [12,13]. The scheme was also extended by the multipartite matrix method which enables one to handle some microstructural effect due to heterogeneity [13].

In principle, to solve the complex thermomechanical problems, all governing equations in the related continuum mechanics must be solved simultaneously because the mechanical fields and the thermodynamic fields are coupled interactively. Accordingly, as summarized in Table. 1, there are three types of mathematical formulation that depend on the treatment of thermomechanically-coupled field variables.

Table. 1   Three types of thermomechanical formulation

Mechanical Fields	Coupling Type (interrelation)	Thermodynamic Fields
stress, strain, viscoplastic strain, displacement, etc.	1. Uncoupled ($\times$) 2. One-way coupled ($\leftarrow$) 3. Fully coupled ($\leftrightarrows$)	temperature, heat flux, energy, entropy, etc.

Theoretical foundations on the thermomechanical coupling phenomena in solid bodies originated from the Duhamel's [14] and the Neumann's [15] paper. It is recognized that the coupling between mechanics and thermodynamics has a weak effect on the behavior of elastic materials, and one-way coupled formulation is sufficient for the thermoelastic problems. But the coupling effect is not always negligible for viscoplastic materials, especially when the materials are repeatedly used under cyclic loads. With the development of viscoplastic deformation, generally, a certain portion of mechanical energy is converted to heat, thus resulting in an irreversible rise in temperature. In result, mechanical variables such as displacement and stress are also changed interactively. Up till now, numerical analyses with the fully-coupled formulation have been performed by several researchers [16-22]. The quantitative prediction of thermomechanical coupling effect in the viscoplastic composites is necessary to accurately analyze the behavior of composite structures operated under intense surrounding conditions.

This paper deals with an issue of the thermomechanically-induced coupling effects on the response of fiber-reinforced composites. The unmixing-mixing scheme is utilized to describe the orthotropic viscoplastic characteristics of the composite materials. The equation of motion and the energy conservation equation are considered together with the constitutive arrangement by the unmixing-mixing concept. By considering auxiliary conditions, the initial-boundary value problem is completely set up. In computational aspects, the governing equations are reformulated with the finite element method. The derived nonlinear equations are fully discretized in incremental forms. As a numerical study, a series of analyses are performed with the focus on the coupling effect in the metal matrix composite. The development of viscoplastic deformation, the stress-strain relation, and the temperature change are carefully examined when the composite laminates are cyclically subjected to static and dynamic loads.

Orthotropic Thermo-Elasto-Viscoplastic Model

Basic Micromechanics

The extended unmixing-mixing scheme with the multipartite matrix method [13] is applied

to describe the thermo-elasto-viscoplastic behavior of composite materials. Some basic equations, which govern the micromechanical states of fiber and matrix, are required for the development of this scheme and they are briefly summarized in this subsection.

(a) Force equilibrium relation

$$\sigma_1 = V_{[f]}\sigma_{[f]1} + \sum_{k=1}^{N} V_{[m_k]}\sigma_{[m_k]1} \tag{1a}$$

$$\sigma_2 = \frac{\sigma_{[f]2}}{p_{[f]2}} = \frac{\sigma_{[m_1]2}}{p_{[m_1]2}} = \cdots = \frac{\sigma_{[m_N]2}}{p_{[m_N]2}} \tag{1b}$$

$$\tau_{12} = \frac{\tau_{[f]12}}{p_{[f]12}} = \frac{\tau_{[m_1]12}}{p_{[m_1]12}} = \cdots = \frac{\tau_{[m_N]12}}{p_{[m_N]12}} \tag{1c}$$

where V denotes the volume fraction. Subscript [f] means the fibers part, and subscript [mi] the i-th matrix part of the N partitioned parts, as shown Fig.1. Another subscripts 1 and 2 denote the principal material coordinates. Also, p2 and p12 are the stress variation factors for the corresponding composite phase.
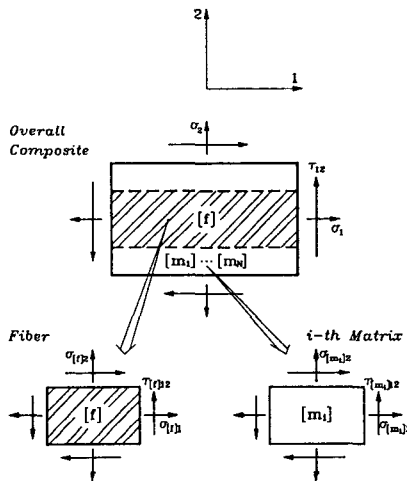

Fig.1 State of force equilibrium in composite materials with a micromechanical viewpoint

(b) Kinematic observation for strain rates

$$\dot{\varepsilon}_1 = \dot{\varepsilon}^e_{[f]1} + \dot{\varepsilon}^t_{[f]1}$$
$$= \dot{\varepsilon}^e_{[m_1]1} + \dot{\varepsilon}^t_{[m_1]1} + \dot{\varepsilon}^p_{[m_1]1}$$
$$= \cdots$$
$$= \dot{\varepsilon}^e_{[m_N]1} + \dot{\varepsilon}^t_{[m_N]1} + \dot{\varepsilon}^p_{[m_N]1} \tag{2a}$$

$$\dot{\varepsilon}_2 = V_{[f]}q_{[f]2}\left(\dot{\varepsilon}^e_{[f]2} + \dot{\varepsilon}^t_{[f]2}\right)$$
$$+ \sum_{k=1}^{N} V_{[m_k]}q_{[m_k]2}\left(\dot{\varepsilon}^e_{[m_k]2} + \dot{\varepsilon}^t_{[m_k]2} + \dot{\varepsilon}^p_{[m_k]2}\right) \tag{2b}$$

$$\dot{\gamma}_{12} = V_{[f]}q_{[f]12}\left(\dot{\gamma}^e_{[f]12} + \dot{\gamma}^t_{[f]12}\right)$$
$$+ \sum_{k=1}^{N} V_{[m_k]}q_{[m_k]12}\left(\dot{\gamma}^e_{[m_k]12} + \dot{\gamma}^t_{[m_k]12} + \dot{\gamma}^p_{[m_k]12}\right) \tag{2c}$$

where superscripts e, t, and p represent the elastic, thermal, and viscoplastic components, respectively. The strain contribution factors q2 and q12 are introduced with the p2 and p12 to account

for the three-dimensional microstructural effects which result from the composite heterogeneity and the kinematic compatibility on interfaces.

(c) Constitutive relation for elastic strains

$$\dot{\varepsilon}^e_{[f]11} = \frac{1}{E_{[f]11}} \dot{\sigma}_{[f]11} - \frac{\nu_{[f]12}}{E_{[f]11}} \dot{\sigma}_{[f]12} \tag{3a}$$

$$\dot{\varepsilon}^e_{[f]12} = \frac{1}{E_{[f]12}} \dot{\sigma}_{[f]12} - \frac{\nu_{[f]12}}{E_{[f]11}} \dot{\sigma}_{[f]11} \tag{3b}$$

$$\dot{\gamma}^e_{[f]112} = \frac{1}{G_{[f]112}} \dot{\tau}_{[f]112} \tag{3c}$$

$$\dot{\varepsilon}^e_{[m_i]11} = \frac{1}{E_{[m]}} \dot{\sigma}_{[m_i]11} - \frac{\nu_{[m]}}{E_{[m]}} \dot{\sigma}_{[m_i]12} \tag{4a}$$

$$\dot{\varepsilon}^e_{[m_i]12} = \frac{1}{E_{[m]}} \dot{\sigma}_{[m_i]12} - \frac{\nu_{[m]}}{E_{[m]}} \dot{\sigma}_{[m_i]11} \tag{4b}$$

$$\dot{\gamma}^e_{[m_i]112} = \frac{2(1+\nu_{[m]})}{E_{[m]}} \dot{\tau}_{[m_i]112} = \frac{1}{G_{[m]}} \dot{\tau}_{[m_i]112} \tag{4b}$$

(d) Constitutive relation for thermal strains

$$\dot{\varepsilon}^t_{[f]11} = \alpha_{[f]11}\,\dot{\theta}_+, \quad \dot{\varepsilon}^t_{[f]12} = \alpha_{[f]12}\,\dot{\theta}_+, \quad \dot{\gamma}^t_{[f]112} = 0 \tag{5}$$

$$\dot{\varepsilon}^t_{[m_i]11} = \alpha_{[m]}\,\dot{\theta}_+, \quad \dot{\varepsilon}^t_{[m_i]12} = \alpha_{[m]}\,\dot{\theta}_+, \quad \dot{\gamma}^t_{[m_i]112} = 0 \tag{6}$$

where α means the coefficient of thermal expansion, and θ_+ is the change from base temperature θ_0 ($\theta = \theta_0 + \theta_+$). It is assumed that θ_+/θ_0 is an infinitesimal of the same order, $O(\varepsilon)$, as the infinitesimal strain tensor ε.

(e) Constitutive relation for matrix viscoplastic strain

Any well-known isotropic viscoplastic theories, which are reviewed in the books by Miller [23] and Lubliner [24], may be used as the matrix viscoplastic model. In this paper, the widely-used constitutive theory proposed by Bodner et al. [25,26] is adopted. The summarized expressions for this rule consist of the flow law, the kinetic equation, and the evolution equations of internal variables (here, no directional hardening is considered).

$$\dot{\varepsilon}^p_{[m_i]} = \lambda\, S_{[m_i]} = \lambda\left[\sigma_{[m_i]} - \frac{1}{3}\,\mathrm{tr}\,(\sigma_{[m_i]})\,1 \right] \tag{7}$$

$$D^p_{[m_i]12} = \frac{1}{2}\,\dot{\varepsilon}^p_{[m_i]} : \dot{\varepsilon}^p_{[m_i]} = D_o^2\,\exp\left(-\frac{Z^{2n}_{[m_i]}}{3^n J^n_{[m_i]12}} \right) \tag{8}$$

$$Z_{[m_i]} = m_1(Z_1 - Z_{[m_i]})\,\sigma^p_{[m_i]} : \dot{\varepsilon}^p_{[m_i]} - A_1 Z_1 \left(\frac{Z_{[m_i]} - Z_2}{Z_1} \right)^{r_1} \tag{9}$$

$$Z_{[m_i]}|_{t=0} = Z_0 \tag{10}$$

where J_2 is the second invariant of the deviatoric stress S, and Z a scalar-valued internal state variable characterizing the isotropic hardening effect. D_o, Z_0, Z_1, Z_2, m_1, A_1, r_1, and n in Eqs. (8)-(10) are the viscoplastic constants for the isotropic matrix.

Derived Unmixing-Mixing Equations

Kim and Shin [13] derived a set of the unmixing-mixing equations by rearranging Eqs. (1)-(6). In this place, only the equations needed in subsequent calculations are rewritten in the appropriate forms.

(a) Strain rate equation

$$\dot{\varepsilon} = \dot{\varepsilon}^e + \dot{\varepsilon}^t + \dot{\varepsilon}^b$$
$$= A \, \dot{\sigma} + a \, \dot{\theta}_+ + \sum_{k=1}^{N} B_{[m_i]} \, \dot{\varepsilon}^b_{[m_k]} \tag{11}$$

where A is the typical elastic compliance tensor under plane-stress condition, and a the thermal expansion tensor. The fourth-order tensor B[mi] relates the viscoplastic deformation of matrix to the overall viscoplastic response of composite by linear transformation. The deformed state in the matrix is represented with a set of variables for the N-parts of the matrix. The matrix forms of these tensors in the 1-2 coordinates are

$$\{\sigma\} = \lfloor \, \sigma_1 \, \sigma_2 \, \tau_{12} \, \rfloor^T, \quad \{\varepsilon\} = \lfloor \, \varepsilon_1 \, \varepsilon_2 \, \gamma_{12} \, \rfloor^T \tag{12}$$

$$[A] = \begin{bmatrix} \dfrac{1}{E_1} & -\dfrac{\nu_{12}}{E_1} & 0 \\ -\dfrac{\nu_{12}}{E_1} & \dfrac{1}{E_2} & 0 \\ 0 & 0 & \dfrac{1}{G_{12}} \end{bmatrix} \tag{13a}$$

$$\{a\} = \lfloor \, a_1 \, a_2 \, 0 \, \rfloor^T \tag{13b}$$

$$[B_{[m_i]}] = V_{[m_i]} \begin{bmatrix} \dfrac{E_{[m]}}{E_1} & 0 & 0 \\ q_{[m_i]2}\nu_{[m]} - \nu_{12}\dfrac{E_{[m]}}{E_1} & q_{[m_i]2} & 0 \\ 0 & 0 & q_{[m_i]12} \end{bmatrix} \tag{13c}$$

The newly appeared notations in Eq.(13) are defined in the following Eqs.(18)-(21).

(b) Fiber-microstress equation

$$\dot{\sigma}_{[f]} = C_{[f]} \, \dot{\sigma} + \beta_{[f]} \, \dot{\theta}_+ + \sum_{k=1}^{N} D_{[f_i]} \, \dot{\varepsilon}^b_{[m_k]} \tag{14}$$

Three terms in the right-hand side of Eq. (14) stand for the fiber-microstress contributed from the overall loading, the thermal expansion, and the matrix viscoplasticity, respectively. The tensors included in the above equations can also be represented by matrix notations.

$$[C_{[f]}] = \begin{bmatrix} \dfrac{E_{[f]1}}{E_1} & \dfrac{V_{[m]}}{E_1} (p_{[f]2}\nu_{[f]12}E_{[m]} - p_{[m]2}\nu_{[m]}E_{[f]1}) & 0 \\ 0 & p_{[f]2} & 0 \\ 0 & 0 & p_{[f]12} \end{bmatrix} \tag{15a}$$

$$\{\beta_{[f]}\} = - V_{[m]} \dfrac{E_{[f]1}E_{[m]}}{E_1} \lfloor \, a_{[f]1} - a_{[m]} \, 0 \, 0 \, \rfloor^T \tag{15b}$$

$$[D_{[f_i]}] = V_{[m_i]} \dfrac{E_{[f]1}}{E_1} \begin{bmatrix} E_{[m]} & 0 & 0 \\ 0 & 0 & 0 \\ 0 & 0 & 0 \end{bmatrix} \tag{15c}$$

(c) Matrix-microstress equation

$$\dot{\sigma}_{[m_i]} = C_{[m_i]} \dot{\sigma} + \beta_{[m]} \dot{\theta}_+ + \sum_{k=1}^{N} D_{[m_{ik}]} \dot{\varepsilon}^p_{[m_k]} \tag{16}$$

$$[C_{[m_i]}] = \begin{bmatrix} \dfrac{E_{[m]}}{E_1} & p_{[m_i]2}\nu_{[m]} - \nu_{12}\dfrac{E_{[m]}}{E_1} & 0 \\ 0 & p_{[m_i]2} & 0 \\ 0 & 0 & p_{[m_i]12} \end{bmatrix} \tag{17a}$$

$$\{\beta_{[m]}\} = V_{[f]}\dfrac{E_{[f]1}E_{[m]}}{E_1} \lfloor \alpha_{[f]1} - \alpha_{[m]} \quad 0 \quad 0 \rfloor^T \tag{17b}$$

$$[D_{[m_{ii}]}] = \left(V_{[m_i]}\dfrac{E_{[m]}}{E_1} - \delta_{ij}\right)\begin{bmatrix} E_{[m]} & 0 & 0 \\ 0 & 0 & 0 \\ 0 & 0 & 0 \end{bmatrix} \tag{17c}$$

(d) Rule of mixtures - elastic modulus

The overall elastic constants in Eqs.(13), (15) and (17) can be expressed in terms of its constituent properties.

$$E_1 = V_{[f]} E_{[f]1} + V_{[m]} E_{[m]} \tag{18a}$$

$$\begin{aligned}
\dfrac{1}{E_2} &= V_{[f]}p_{[f]2}q_{[f]2}\dfrac{1}{E_{[f]2}} + V_{[m]}\widetilde{pq}_{[m]2}\dfrac{1}{E_{[m]}} \\
&\quad + V_{[f]}V_{[m]}\{ (p_{[f]2}q_{[m]2} + p_{[m]2}q_{[f]2})\nu_{[f]12}\nu_{[m]} \\
&\quad - p_{[f]2}q_{[f]2}\nu_{[f]12}^2\dfrac{E_{[m]}}{E_{[f]1}} - \widetilde{pq}_{[m]2}\nu_{[m]}^2\dfrac{E_{[f]1}}{E_{[m]}} \}\dfrac{1}{E_1} \\
&\quad + V_{[m]}^2(p_{[m]2}q_{[m]2} - \widetilde{pq}_{[m]2})\nu_{[m]}^2\dfrac{1}{E_1}
\end{aligned} \tag{18b}$$

$$\nu_{12} = V_{[f]}p_{[f]2}\nu_{[f]12} + V_{[m]}p_{[m]2}\nu_{[m]} \tag{18c}$$

$$\widetilde{\nu}_{12} = V_{[f]}q_{[f]2}\nu_{[f]12} + V_{[m]}q_{[m]2}\nu_{[m]} \tag{18d}$$

$$\dfrac{1}{G_{12}} = V_{[f]}p_{[f]12}q_{[f]12}\dfrac{1}{G_{[f]12}} + V_{[m]}\widetilde{pq}_{[m]12}\dfrac{1}{G_{[m]}} \tag{18e}$$

These equations are derived with the context of the unmixing-mixing scheme, and regarded as the extension of the traditional rule of mixtures illustrated in the textbooks on composite mechanics [27,28].

(e) Rule of mixtures - coefficient of thermal expansion

$$\alpha_1 = V_{[f]}\dfrac{E_{[f]1}}{E_1}\alpha_{[f]1} + V_{[m]}\dfrac{E_{[m]}}{E_1}\alpha_{[m]} \tag{19a}$$

$$\begin{aligned}
\alpha_2 &= V_{[f]}q_{[f]2}\alpha_{[f]2} + V_{[m]}q_{[m]2}\alpha_{[m]} \\
&\quad + V_{[f]}V_{[m]}\left(q_{[f]2}\nu_{[f]12}\dfrac{E_{[m]}}{E_1} - q_{[m]2}\nu_{[m]}\dfrac{E_{[f]1}}{E_1}\right)(\alpha_{[f]1} - \alpha_{[m]})
\end{aligned} \tag{19b}$$

(f) Other notation and constraint

In the above equations, the following abbreviated notations are used for convenience.

$$V_{[m]} = \sum_{k=1}^{N} V_{[m_k]}, \quad V_{[f]} + V_{[m]} = 1 \tag{20}$$

$$p_{[m]2} = \sum_{k=1}^{N} V_{[m_k]} p_{[m_k]2} \bigg/ V_{[m]}$$

(21a)

$$q_{[m]2} = \sum_{k=1}^{N} V_{[m_k]} q_{[m_k]2} \bigg/ V_{[m]}$$

(21b)

$$\overline{pq}_{[m]2} = \sum_{k=1}^{N} V_{[m_k]} p_{[m_k]2} q_{[m_k]2} \bigg/ V_{[m]}$$

(21c)

$$\overline{pq}_{[m]12} = \sum_{k=1}^{N} V_{[m_k]} p_{[m_k]12} q_{[m_k]12} \bigg/ V_{[m]}$$

(21d)

In addition, the constraint requirements that the averaged states of the stress components should be equilibrated in the composite material yields the following relationships in terms of volume fractions and stress variation factors.

$$V_{[f]} p_{[f]2} + \sum_{k=1}^{N} V_{[m_k]} p_{[m_k]2} = 1$$

(22a)

$$V_{[f]} p_{[f]12} + \sum_{k=1}^{N} V_{[m_k]} p_{[m_k]12} = 1$$

(22b)

The reciprocal theorem in elasticity must be satisfied as well, so yielding

$$\nu_{12} = \overline{\nu}_{12}$$

(23)

Governing Equations and Auxiliary Conditions

In this section, governing equations are briefly summarized in tensor notation. As shown in Fig.2, the thin laminates which infinitesimally deform in a plane are considered.
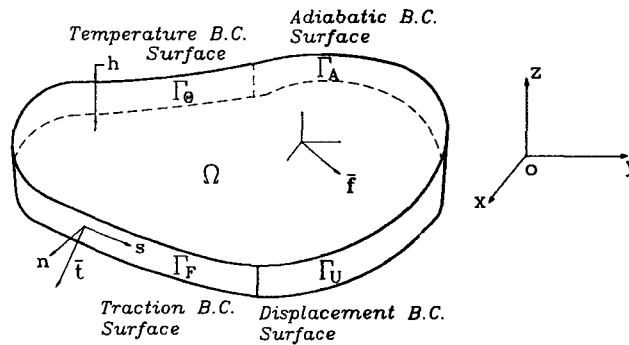

Fig.2   Geometric configuration of a composite laminate and its boundaries

(a) Equation of motion

$$\nabla \cdot \sigma + \overline{f} = \rho \ddot{u}$$

(24)

(b) Energy conservation equation

By applying the principles of thermodynamics (energy conservation and entropy production) [29], Eq.(25) is derived for a class of viscoplastic composites.

$$\rho c_v \theta_+ = -\theta \, a : A^{-1} : (\dot{\varepsilon} - \dot{\varepsilon}^p) + \xi \sigma : \dot{\varepsilon}^p + \nabla \cdot (x \cdot \nabla \theta_+)$$

(25)

The terms in the right-hand side are the contribution to thermal energy by the reversible thermoelastic deformation, the dissipative viscoplastic deformation, and the irreversible heat conduction, respectively.

(c) Strain-displacement relation

$$\varepsilon = \frac{1}{2} [\nabla \cdot u + (\nabla \cdot u)^T] \tag{26}$$

(d) Constitutive equation ; unmixing-mixing scheme

The following are the extended unmixing-mixing equations illustrated in the previous section ; that is, the strain rate equation, the overall viscoplastic flow law, the fiber stress equation, and the matrix stress equation.

$$\dot{\varepsilon} = A \dot{\sigma} + a \dot{\theta}_+ + \dot{\varepsilon}^p \tag{27}$$

$$\dot{\varepsilon}^p = \sum_{k=1}^{N} B_{[m_k]} \dot{\varepsilon}^p_{[m_k]} \tag{28}$$

$$\dot{\sigma}_{[f]} = C_{[f]} \dot{\sigma} + \beta_{[f]} \dot{\theta}_+ + \sum_{k=1}^{N} D_{[f_k]} \dot{\varepsilon}^p_{[m_k]} \tag{29}$$

$$\dot{\sigma}_{[m_i]} = C_{[m_i]} \dot{\sigma} + \beta_{[m]} \dot{\theta}_+ + \sum_{k=1}^{N} D_{[m_{ik}]} \dot{\varepsilon}^p_{[m_k]} \tag{30}$$

(e) Constitutive equation ; Bodner-Partom theory

$$\dot{\varepsilon}^p_{[m_i]} = \frac{D_o}{\sqrt{J_{[m_i]2}}} \exp\left[-\frac{1}{2}\left(\frac{Z^2_{[m_i]}}{3J_{[m_i]2}}\right)^n \right] S_{[m_i]} \tag{31}$$

$$S_{[m_i]} \overset{\text{def}}{=} \sigma_{[m_i]} - \frac{1}{3} \operatorname{tr}(\sigma_{[m_i]}) 1 \tag{32}$$

$$J_{[m_i]2} \overset{\text{def}}{=} \frac{1}{2} S_{[m_i]} : S_{[m_i]} \tag{33}$$

$$\dot{Z}_{[m_i]} = m_1(Z_1 - Z_{[m_i]}) \sigma_{[m_i]} : \dot{\varepsilon}^p_{[m_i]} - A_1 Z_1 \left(\frac{Z_{[m_i]} - Z_2}{Z_1}\right)^{r_1} \tag{34}$$

The detailed information on unknowns and equations is listed in Table. 2. By prescribing auxiliary conditions together, the initial-boundary value problem is completely defined.

(a) Initial condition ; macromechanical variables

$$\sigma|_{t=0} = 0, \quad \varepsilon|_{t=0} = 0, \quad \varepsilon^p|_{t=0} = 0 \tag{35}$$

$$u|_{t=0} = 0, \quad \dot{u}|_{t=0} = 0, \quad \theta_+|_{t=0} = 0 \tag{36}$$

(b) Initial condition ; micromechanical variables

$$Z_{[m_i]}|_{t=0} = Z_0, \quad other \ variables = 0 \tag{37}$$

(c) Displacement boundary condition

$$u = \overline{u} \quad on \ \Gamma_U \tag{38}$$

(d) Traction boundary condition

$$n \cdot \sigma = \overline{t} \quad on \ \Gamma_F \tag{39}$$

(e) Temperature boundary condition

$$\theta_+ = \bar{\theta}_+ \quad on \ \Gamma_\theta \tag{40}$$

(f) Adiabatic boundary condition

$$(x \cdot \nabla\theta_+) \cdot n = 0 \quad on \ \Gamma_A \tag{41}$$

Table. 2 List of unknowns and equations

Unknowns		Equations		
Macro-Level Variable		Eqn of Motion	; (24)	2
		Energy Conservation Eqn	; (25)	1
Stress Tensor	3	Strain-Displacement Relation	; (26)	3
Strain Tensor	3			
Displacement Vector	2	Constitutive Eqn		
Temperature	1	(Unmixing-Mixing Scheme)		
Viscoplastic Strain Tensor	3	Strain Rate Eqn	; (27)	3
		Viscoplastic Flow Law	; (28)	3
Micro-Level Variable		Fiber Stress Eqn	; (29)	3
Fiber Stress Tensor	3	Matrix Stress Eqn	; (30)	N×3
Matrix Stress Tensor	N×3	Constitutive Eqn		
Matrix Deviatoric Stress Tensor	N×4	(Bodner-Partom Theory)		
Matrix Viscoplastic Strain Tensor	N×3	Flow Law and Kinetic Eqn	; (31)	N×3
Matrix Deviatoric Stress Invariant	N	Deviatoric Stress Definition	; (32)	N×4
Matrix Internal State Variable	N	Stress Invariant Definition	; (33)	N
		Evolution Eqn	; (34)	N
Total → 15+N×12		Total → 15+N×12		

Variational Formulation and Finite Element Approximation

Equation of Motion

Variational formulation starting from governing differential equations is performed in order to solve the fully-coupled problems. The principle of virtual work is applied to the equilibrium state with the virtual displacement which vanishes on Γ_U.

$$\int_\Omega (\nabla \cdot \sigma + \bar{f} - \rho\ddot{u}) \cdot \delta u \, d\Omega - \int_{\Gamma_F} (n \cdot \sigma - \bar{t}) \cdot \delta u \, d\Gamma_F = 0 \tag{42}$$

The displacement and the temperature are spatially interpolated with the isoparametric finite elements.

$$\begin{Bmatrix} u(x,y;t) \\ v(x,y;t) \end{Bmatrix} = [H_U(x,y)]\{U(t)\} \tag{43}$$

$$\begin{Bmatrix} \varepsilon_x(x,y;t) \\ \varepsilon_y(x,y;t) \\ \gamma_{xy}(x,y;t) \end{Bmatrix} = [B_U(x,y)]\{U(t)\} \tag{44}$$

$$\theta_+(x,y;t) = [H_\theta(x,y)]\{\Theta(t)\} \tag{45}$$

$$\left\{ \begin{array}{c} \dfrac{\partial \theta_+}{\partial x}(x,y;t) \\[2mm] \dfrac{\partial \theta_+}{\partial y}(x,y;t) \end{array} \right\} = [B_\theta(x,y)]\{\Theta(t)\} \tag{46}$$

By using the divergence theorem, the semi-discretized form of the equation of motion can be derived as follows :

$$[M_U]\{\ddot{U}\} + \{F_U\} - \{R_U\} = \{0\} \tag{47}$$

where

$$[M_U] \triangleq \int_\Omega \rho [H_U]^T [H_U] \, d\Omega \tag{48}$$

$$\{F_U\} \triangleq \int_\Omega [B_U]^T \{\sigma\} \, d\Omega \tag{49}$$

$$\{R_U\} \triangleq \int_\Omega [H_U]^T \{\bar{f}\} \, d\Omega + \int_{\Gamma_F} [H_U]^T \{\bar{t}\} \, d\Gamma_F \tag{50}$$

To obtain a fully-discretized approximation, the Newmark integration (constant average acceleration) method [30] is applied to Eq.(47). It is noted that the temperature vector is a secondary independent variable in the above equations.

$$\left([K_U] + \frac{4}{\Delta t^2}[M_U]\right)\{\Delta U\} = \{^{t+\Delta t}R_U\} - \{^t F_U\}$$
$$+ [A_\theta]\{\Delta\Theta\} + \{\Delta P_U\} + [M_U]\left(\frac{4}{\Delta t}\{^t\dot{U}\} + \{^t\ddot{U}\}\right) \tag{51}$$

$$[K_U] \triangleq \int_\Omega [B_U]^T [A]^{-1} [B_U] \, d\Omega \tag{52}$$

$$[A_\theta] \triangleq \int_\Omega [B_U]^T [A]^{-1} \{a\} [H_\theta] \, d\Omega \tag{53}$$

$$\{\Delta P_U\} \triangleq \int_\Omega [B_U]^T [A]^{-1} \{\Delta \varepsilon^p\} \, d\Omega \tag{54}$$

$$\{\Delta \varepsilon^p\} \triangleq \int_t^{t+\Delta t} \{\dot{\varepsilon}^p\} \, d\tau \tag{55}$$

Energy Conservation Equation

Next, the Galerkin method is used for the restatement of the energy conservation equation.

$$\int_\Omega \rho c_v \dot{\theta}_+ \delta\theta \, d\Omega - \int_\Omega \nabla \cdot (\boldsymbol{x} \cdot \nabla \theta_+) \delta\theta \, d\Omega$$
$$= -\int_\Omega \theta \, \boldsymbol{a} : A^{-1} : (\dot{\varepsilon} - \dot{\varepsilon}^p) \delta\theta \, d\Omega + \int_\Omega \xi \, \sigma : \dot{\varepsilon}^p \delta\theta \, d\Omega \tag{56}$$

Through the procedure of finite element discretization, the following is obtained.

$$[M_\theta]\{\dot{\Theta}\} + [K_\theta]\{\Theta\} = \{E_\theta\} + \{P_\theta\} \tag{57}$$

where

$$[M_\theta] \triangleq \int_\Omega \rho c_v [H_\theta]^T [H_\theta] \, d\Omega \tag{58}$$

$$[K_\theta] \triangleq \int_\Omega [B_\theta]^T [x] [B_\theta] \, d\Omega \tag{59}$$

$$\{E_\theta\} \triangleq - \int_\Omega \theta [H_\theta]^T \{a\}^T [A]^{-1} (\{\dot\varepsilon\} - \{\dot\varepsilon^p\}) \, d\Omega \tag{60}$$

$$\{P_\theta\} \triangleq \int_\Omega \xi [H_\theta]^T \{\sigma\}^T \{\dot\varepsilon^p\} \, d\Omega \tag{61}$$

Eq.(57) is fully discretized with the Crank-Nicolson technique [31] in a time domain.

$$\left([M_\theta] + \frac{\Delta t}{2} [K_\theta] \right) \{\Delta\Theta\} = \{\Delta E_\theta\} + \{\Delta P_\theta\} - \Delta t [K_\theta] \{{}^t\Theta\} \tag{62}$$

$$\{\Delta E_\theta\} \triangleq - \int_\Omega [H_\theta]^T \{a\}^T [A]^{-1} \{\Delta\bar\varepsilon\} \, d\Omega \tag{63}$$

$$\{\Delta P_\theta\} \triangleq \int_\Omega \xi [H_\theta]^T \{\Delta w^p\} \, d\Omega \tag{64}$$

$$\{\Delta\bar\varepsilon\} \triangleq \int_t^{t+\Delta t} \theta (\{\dot\varepsilon\} - \{\dot\varepsilon^p\}) \, d\tau \tag{65}$$

$$\{\Delta w^p\} \triangleq \int_t^{t+\Delta t} \{\sigma\}^T \{\dot\varepsilon^p\} \, d\tau \tag{66}$$

Computational Algorithm

The resulting equations, Eq.(51) and (62), are nonlinear with the fully-coupled terms. Therefore, the incremental solutions, $\{\Delta U\}$ and $\{\Delta\Theta\}$, are obtained through an iteration process. The fast convergence depends largely on how accurately the nonlinear terms in Eq.(55), (65), and (66) are calculated. Because of the numerically stiff phenomenon of the viscoplastic rate equations, a subincrementing technique is adopted at each Gauss integration point [32]. The computational algorithm for the finite element code is as follows :

(a) Initialize all the variables at $t=0$, and determine Δt.
(b) Apply the load increment, and start the iteration stage with $i=0$.
(c) Assemble the matrices in Eq.(51), and solve it to obtain $\{^{(i+1)}\Delta U\}$.
(d) Calculate the nonlinear terms in the energy equation by the subincrementing technique.

$$\{^{(i)}\Delta\bar\varepsilon\} = \int_t^{t+\Delta t} {}^{(i)}\theta (\{^{(i)}\varepsilon\} - \{^{(i)}\dot\varepsilon^p\}) \, d\tau \tag{67}$$

$$\{^{(i)}\Delta w^p\} = \int_t^{t+\Delta t} \{^{(i)}\sigma\}^T \{^{(i)}\dot\varepsilon^p\} \, d\tau \tag{68}$$

(e) Assemble the matrices in Eq.(62), and solve it to obtain $\{^{(i+1)}\Delta\Theta\}$.
(f) Calculate the nonlinear term in the equation of motion by the subincrementing technique.

$$\{^{(i)}\Delta\varepsilon^p\} = \int_t^{t+\Delta t} \{^{(i)}\dot\varepsilon^p\} \, d\tau \tag{69}$$

(g) Check the convergence criteria with the relative errors.
(h) If it converges, update all the variables to the current values. Return to (b).
(i) If it diverges, increase the iteration index i by one. Return to (c).

With a slight modification, the above algorithm can be applied to other problems. For example, if the steps of (d) and (e) are skipped, the uncoupled structural analysis can be performed. And by neglecting (c) and (f), the equation of unsteady heat conduction for composite laminates can be solved.

Numerical Examples and Discussion

Metal Matrix Composite

The metal matrix composite, SCS-6/Ti-15-3 (silicon-carbide fiber, titanium alloy matrix), is selected as the standard material system in numerical analyses. The material properties are chosen at a high temperature, 815°C [22]. The fiber volume fraction is 0.6, and the unmixing-mixing model has one part of fiber and two parts of matrix ($V_{[m1]}$ = 0.3, $V_{[m2]}$ = 0.1). The typical stress-strain curves are shown in Fig.3.
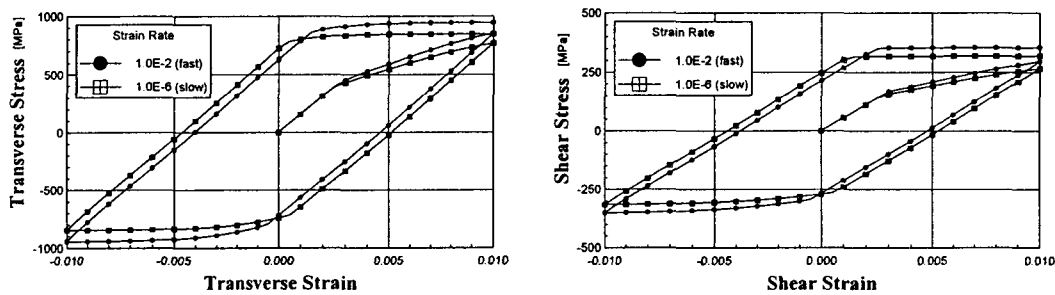

Fig.3 $\sigma_2 - \varepsilon_2$ and $\tau_{12} - \gamma_{12}$ curves for SCS-6/Ti-15-3

Uniform Field Problem ; Off-Axis Specimen

As shown in Fig.4., we consider a fiber-reinforced composite subject to uniaxial loading at angle λ to the fiber direction. Since the macroscopically homogenized composite is under static uniform loads, the equation of motion is not solved. And the heat conduction term resulting from the temperature gradient can be neglected in the energy equation.
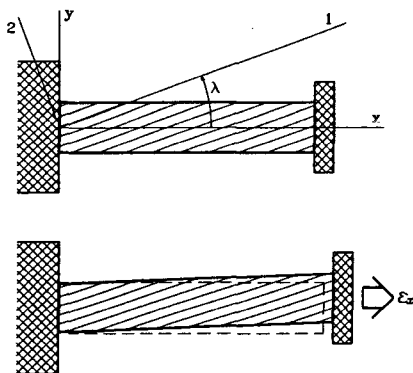

Fig.4 Insulated composite specimen
with off-axis angle λ

Through the transformation equations for expressing the stresses and strains in the 1-2 coordinates in terms of the stresses and strains in an x-y coordinates, the rate equations for unknown quantities σ_x, ε_y, γ_{xy}, and θ_+ are derived. Eq.(70) is a system of nonlinear, first-order differential equations. One-step forward Euler method appears to be suitable for the simple and efficient time integration, provided the time step is finely divided.

$$
\begin{bmatrix}
1/E_x & 0 & 0 & \alpha_x \\
\nu_{xy}/E_x & 1 & 0 & -\alpha_y \\
-\eta_{xy,x}/E_x & 0 & 1 & -\alpha_{xy} \\
0 & \alpha_y & \alpha_{xy} & \rho c_v
\end{bmatrix}
\begin{Bmatrix}
\dot{\sigma}_x \\
\dot{\epsilon}_y \\
\dot{\gamma}_{xy} \\
\dot{\theta}_+
\end{Bmatrix}
=
\begin{Bmatrix}
\dot{\epsilon}_x - \dot{\epsilon}_x^p \\
\dot{\epsilon}_y^p \\
\dot{\gamma}_{xy}^p \\
-\overline{\alpha}_x \dot{\epsilon}_x + (\overline{a}_1 \dot{\epsilon}_1^p + \overline{a}_2 \dot{\epsilon}_2^p) + \xi \sigma_x \dot{\epsilon}_x^p
\end{Bmatrix}
\tag{70}
$$

The various components in Eq.(70) can be written as follows.

$$
\frac{1}{E_x} = \frac{1}{E_1}\cos^4\lambda + \left(\frac{1}{G_{12}} - \frac{2\nu_{12}}{E_1}\right)\cos^2\lambda \sin^2\lambda + \frac{1}{E_2}\sin^4\lambda
\tag{71a}
$$

$$
\frac{\nu_{xy}}{E_x} = \frac{\nu_{12}}{E_1}(\cos^4\lambda + \sin^4\lambda) - \left(\frac{1}{E_1} + \frac{1}{E_2} - \frac{1}{G_{12}}\right)\cos^2\lambda \sin^2\lambda
\tag{71b}
$$

$$
\frac{\eta_{xy,x}}{E_x} = \left(\frac{2}{E_1} + \frac{2\nu_{12}}{E_1} - \frac{1}{G_{12}}\right)\cos^3\lambda \sin\lambda - \left(\frac{2}{E_2} + \frac{2\nu_{12}}{E_1} - \frac{1}{G_{12}}\right)\cos\lambda \sin^3\lambda
\tag{71c}
$$

$$
\alpha_x = a_1 \cos^2\lambda + a_2 \sin^2\lambda
\tag{72a}
$$

$$
\alpha_y = a_1 \sin^2\lambda + a_2 \cos^2\lambda
\tag{72a}
$$

$$
\alpha_{xy} = 2(a_1 - a_2)\cos\lambda \sin\lambda
\tag{72c}
$$

$$
\overline{a}_1 = \theta_o(a_1 Q_{11} + a_2 Q_{12})
\tag{73a}
$$

$$
\overline{a}_2 = \theta_o(a_1 Q_{12} + a_2 Q_{22})
\tag{73b}
$$

$$
\overline{\alpha}_x = \overline{a}_1 \cos^2\lambda + \overline{a}_2 \sin^2\lambda
\tag{74a}
$$

$$
\overline{\alpha}_y = \overline{a}_1 \sin^2\lambda + \overline{a}_2 \cos^2\lambda
\tag{74b}
$$

$$
\overline{\alpha}_{xy} = (\overline{a}_1 - \overline{a}_2)\cos\lambda \sin\lambda
\tag{74c}
$$

where Q_{11}, Q_{12}, and Q_{22} are the so-called reduced stiffness components.

Fig.5 illustrates the typical results of the temperature variations up to 1,200s for the off-axis angle $\lambda = 30°$. The ε_{max} varies from 0.003 to 0.006. With the increased ε_{max}, the variations in the temperature curves are noticeable. The general trends of temperature variations depend mainly on the hysteretic areas in the stress-strain curves, which is a measure of plastic deformation in one cycle. The values of the temperature change θ_+ are over 10°C after ten cycles in case of $\varepsilon_{max} = 0.006$.
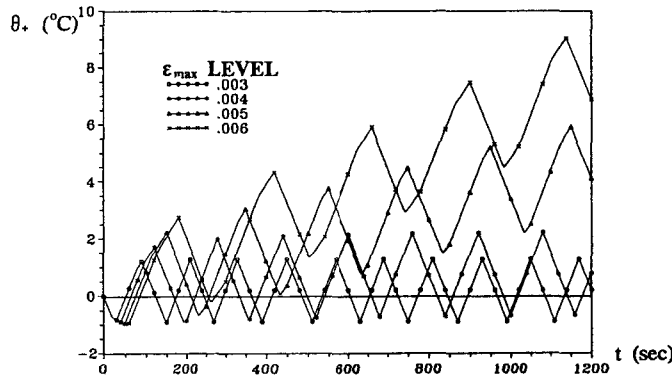

Fig.5 θ_+ time histories for various ε_{max} levels

To examine the thermomechanical coupling effects on the temperature changes quantitatively, the relations $\theta_+|_{max}$ - $\theta_+|_{min}$ versus λ are graphed with various ε_{max} levels in Fig.6. In the figure, $\theta_+|_{max}$ is the maximum temperature change in the entire loading history up to N_c=20, and $\theta_+|_{min}$ the minimum. N_c=20 means the well-developed stage at which the dissipated plastic work plays a dominant role.
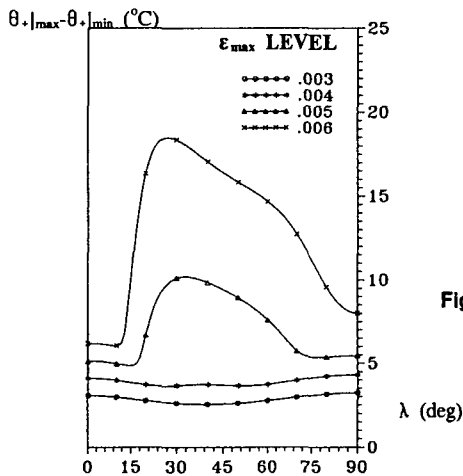

Fig.6 $\theta_{+|max}$-$\theta_{+|min}$ vs λ (N_c=20)

Nonuniform Field Problem ; Quasistatics

The intial-boundary value problems with nonuniform field variables are examined with the developed computer code. As shown in Fig.7, the square laminate has the length a, and the hole is located in the center with the radius R. The stacking sequence of the composite laminate is [0/±45/90]s, and the traction loads are along the x-axis. Considering the geometric and material symmetry, a quarter of the laminate is discretized by 1680 triangular finite elements.
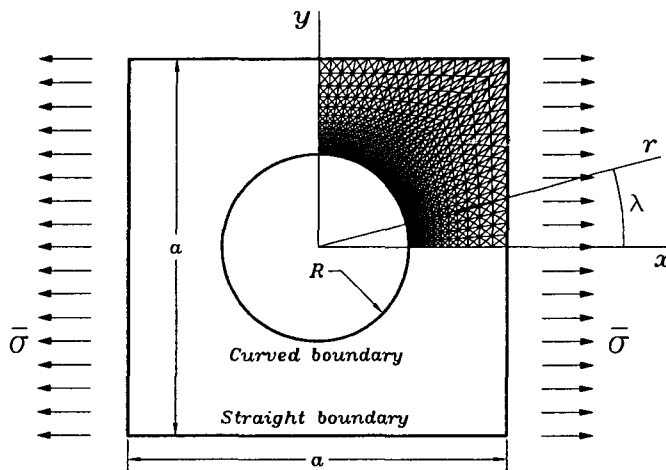

Fig.7 Configuration of the composite laminate with a hole

Traction force is tension, unloading, compression, and unloading (T,U,C,U) during tc for one cycle, as shown in Fig.8. The upper bound of the cyclic load is 225MPa and the lower bound -225MPa. A total of five examples are tested to compare the fully-coupled quasistatic solutions with each other, as listed in Table. 3. The size of the laminate is a=4.0m and R=1.0m in STAT1~STAT3, a=0.4m and R=0.1m in STAT4, and a=0.04m and R=0.01m in STAT5. In addition, the load period is different in each case.
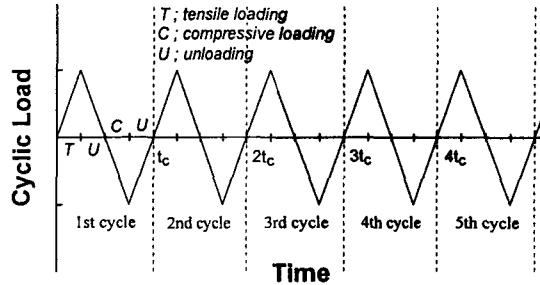
Fig.8   Time history of cyclic loading applied to a composite laminate

Table. 3   Numerical tests for quasistatic loading

	t_c [s]	σ_{max} [MPa]	a [m]	R [m]
STAT1	4.00	±225	4.00	1.00
STAT2	40.0	±225	4.00	1.00
STAT3	400.	±225	4.00	1.00
STAT4	4.00	±225	0.40	0.10
STAT5	4.00	±225	0.04	0.01

Contour maps are drawn to view the distribution of viscoplastic work accumulated in the laminae. Fig.9 is the developed work during 0~1s. The maximum value is predicted at the upper boundary of the hole in the 90° ply. Note that the dissipated viscoplastic work is one measure of the heating effect owing to thermomechanical coupling. It is expected that the coupling effect may become apparent around the upper boundary of the hole.
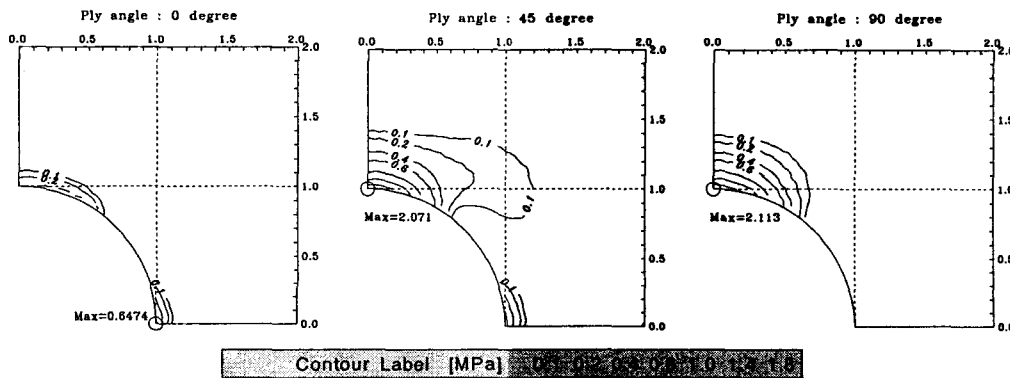

Fig.9   Developed viscoplastic work during 0~1s (1st cycle) ; STAT1

To examine the thermomechanical coupling effect, the temperature changes from the base temperature θ_0 are predicted at a boundary point during the first four cycles. In Fig.10, the cycle number is a dimensionless parameter of the current time t with reference to t_c. Because the laminates deform viscoplastically around the point, the upper bounds of temperature values increase gradually, except in STAT5.
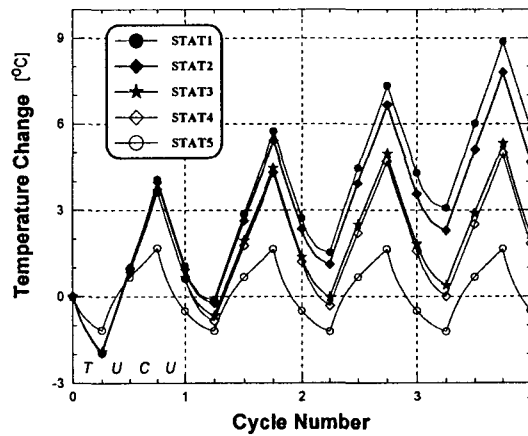

Fig.10   Temperature change vs. cycle number (t/t_c) up to the 4th cycle at $(r,\lambda)=(R,90°)$

Fig.11 shows the distribution of the temperature change θ_+ along hole boundary. The patterns of the temperature distribution are different for each problem. They depend mainly on heat conduction term in the energy conservation equation. If the load is applied at a higher rate, the viscoplastic work will be accumulated on a local area with less heat conduction. Therefore, the local heating effect lasts as in STAT1 or STAT2. The maximum temperature change is about 30°C. When the number of the repeated cycles is increased, the heating effect will be considerable. In contrast to these cases, the heating effect is relatively weak in STAT3 because of slower loading. By drawing a comparison between STAT1, STAT4, and STAT5, one can see that the laminate size also plays an important role. The coupling effect is negligible for a small laminate as in STAT5, because the thermal energy easily spreads to the surrounding.
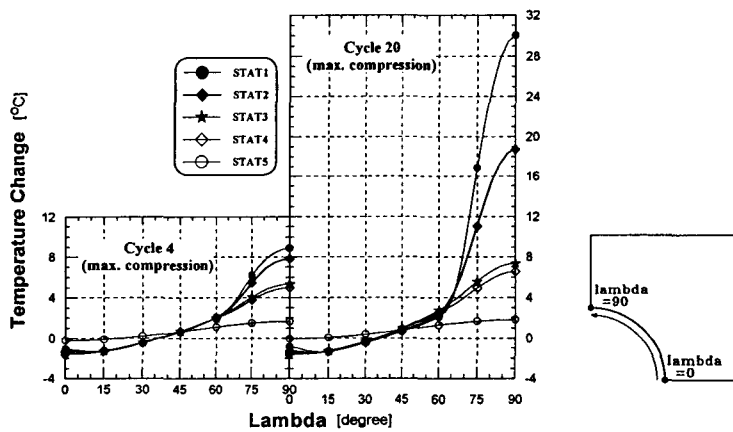

Fig.11   Distribution of temperature change at t/t_c=3.75 and 19.75 (max. compression)

Nonuniform Field Problem ; Dynamics

When the t_c has the same order as the fundamental period t_n for the initial elastic state of the composite laminate, dynamic analyses must be performed including the inertia term. As shown in Fig.12, consider a laminate supported by rigid walls with the dimension, $a=1.0$m, $b=0.09$m, and $h=0.01$m. The stacking sequence is $[0/\pm45/90]_s$. Only the right half is discretized with 480 triangular elements. The point force is cyclically applied with the range of $\pm P_{max}$, as shown in Fig.8.
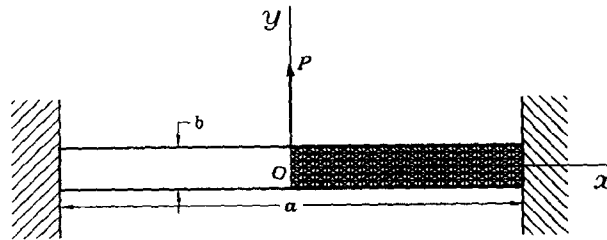
Fig.12 Configuration of the composite laminate supported by rigid walls

The fundamental period can be determined by solving the generalized eigenvalue problem of the free vibration for the elastic deformation.

$$[K_U]\{\phi\} = \omega^2[M_U]\{\phi\} \tag{75}$$

Because only the lower modes need to be checked, the natural mode shapes for the four modes are shown in Fig.13 with their periods $2\pi/\omega$. Note that the fundamental period is equal to 1.566ms.
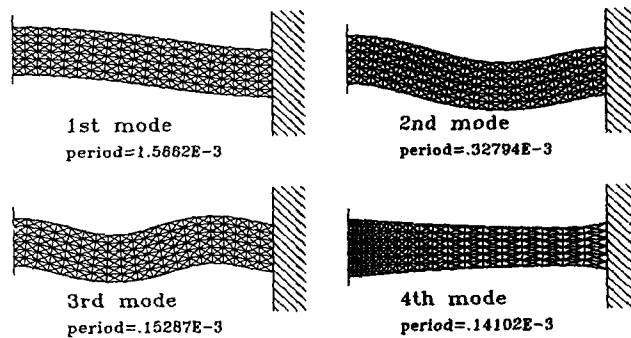
1st mode
period=1.5882E-3

2nd mode
period=.32794E-3

3rd mode
period=.15287E-3

4th mode
period=.14102E-3

Fig.13 Natural mode shapes and periods of the composite laminate

Two examples are solved to show the coupled dynamic behavior of the viscoplastic composite. Because the fundamental mode is important in this case, t_c is changed with reference to t_n. In DYNA1, the load cycle t_c is 7.831ms, five times of the t_n, with $P_{max}=195.8$kN. In DYNA2, the t_c is equal to t_n with $P_{max}=35.24$kN. In numerical experiments, the relative errors for convergence are fixed to 0.02%, and the subdivision number for the subincrementing technique is 100.

DYNA1 results are presented in Fig.14~Fig.16. In Fig.14, the deflection at the center of laminate is plotted with the cycle number. In the legend of the figure, T.E. designates thermo-elasticity,

and T.E.VP. thermo-elasto-viscoplasticity. The curve of quasistatic (Q) T.E.VP. is also drawn to observe the characteristics of dynamic (D) T.E.VP. The deflection curve of Q.T.E.VP. linearly increases or decreases with constant amplitude, which implies that no viscoplastic deformation occurs. The result of D.T.E. means that the deflection steadily grows owing mainly to the component of the first natural mode (the component of the first mode oscillates about five times per cycle). But the curve of D.T.E.VP. is a contrast to these curves.
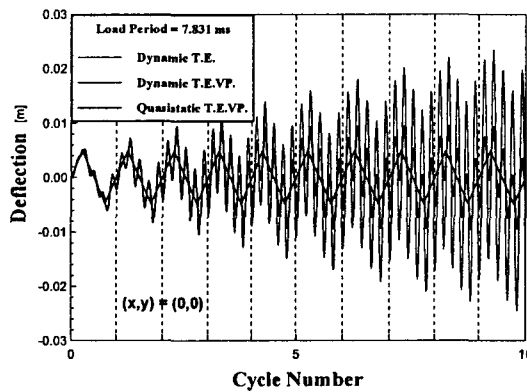

Fig.14   Deflection vs. cycle number (t / t_c) up to the 10th cycle at (x,y)=(0,0) ; DYNA1

Though the difference between them is not obvious at the initial stage, the difference becomes outstanding after the third cycle as the viscoplastic deformation develops. Note that the viscoplastic deformation provides the source of damping in the thermomechanical system, so the range of deflection is confined within about 0.01m.

To visualize the viscoplastic deformation in the laminate, as shown in Fig.15, the contour maps of viscoplastic work per unit volume are drawn at $t=10t_c$. A considerable amount of the irreversible work is developed in the upper and the lower area of the center and the right boundaries, mainly because the normal stress σ_x is large in those regions. The other parts of the laminate deform elastically. The viscoplastic deformation dissipates mechanical energy into thermal energy, so the dynamic motion of the laminate does not diverge.
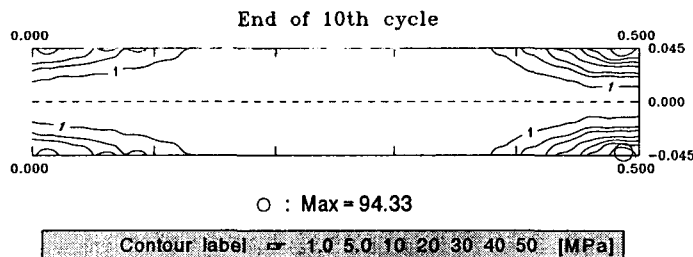

Fig.15   Developed viscoplastic work at t=10.0t_c ; DYNA1

The response of temperature change due to the coupling effect is shown in Fig.16. The result of D.T.E. shows that the phases of heating and cooling are repeated proportionally to the deflection without any viscoplastic effect. The heating effect is serious in the D.T.E.VP. case. The maximum temperature change is about 30°C in the tenth cycle. This confirms the fact that, to constrain a divergent motion, viscoplastic work is transformed to thermal energy which is accumulated
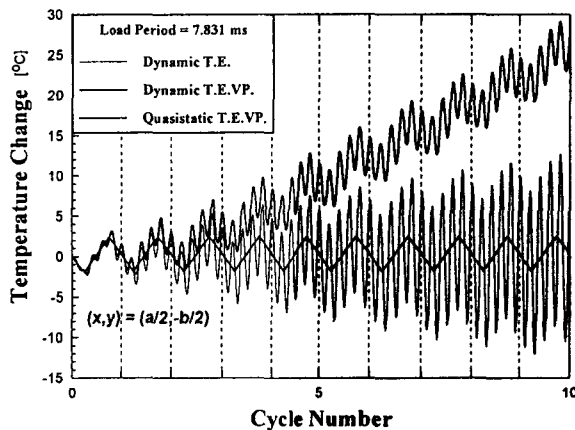
in the insulated system.

Fig.16   Temperature change vs. cycle number (t/t_o) up to the 10th cycle at $(x,y)=(a/2,-b/2)$; DYNA1

Finally, the temperature response of DYNA2 is plotted in Fig.17. As expected, the coupling effect is noticeable for the D.T.E.VP. curve. The maximum temperature rise is about $25^\circ C$ after the ten cycles.
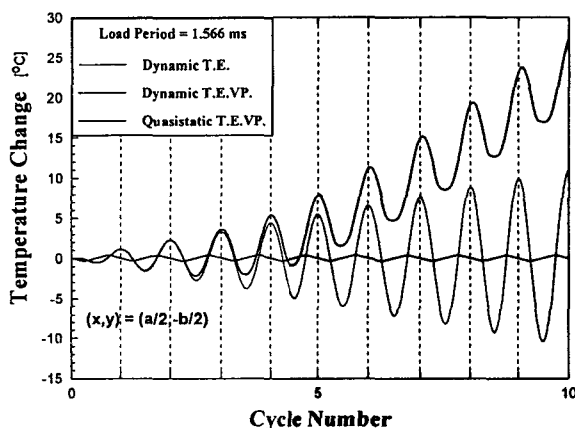

Fig.17   Temperature change vs. cycle number (t / t_o) up to the 10th cycle at $(x,y)=(a/2,-b/2)$; DYNA2

Conclusions

In this paper, we set up the finite element formulation that enables thermo-elasto-viscoplastic analyses for composite materials focusing on the fully-coupled thermomechanical situation. The matrix-partitioned unmixing-mixing scheme was adopted as the constitutive model on orthotropic thermo-elasto-viscoplasticity. Through a series of numerical tests, it is concluded that the heating effect due to the irreversible viscoplastic work may be significant depending on the repeated cycles,

the applied load levels, and the material properties. In quasistatic nonuniform field problems, especially, the thermal conduction in the energy equation can relieve the cyclic heating effect. On the other hand, in dynamic environment, the viscoplastic work dissipates mechanical energy into thermal energy, which plays the role of a damping mechanism.

References

[1]Tenney, D. R., Lisagor, W. B., and Dixon, S. C., "Materials and Structures for Hypersonic Vehicles," *Journal of Aircraft*, Vol. 26, No. 11, 1989, pp. 953-970.

[2]*Thermal Structures and Materials for High-Speed Flight*, edited by E. A. Thornton, Vol. 140, Progress in Astronautics and Aeronautics, AIAA, Washington, DC, 1992.

[3]Robinson, D. N., and Duffy, S. F., "Continuum Deformation Theory for High-Temperature Metallic Composites," *Journal of Engineering Mechanics*, Vol. 116, No. 4, 1990, pp. 832-844.

[4]Lee, K. D., and Krempl, E., "An Orthotropic Theory of Viscoplasticity Based on Overstress for Thermomechanical Deformations," *International Journal of Solids and Structures*, Vol. 27, No. 11, 1991, pp. 1445-1459.

[5]Gates, T. S., and Sun, C. T., "Elastic/Viscoplastic Constitutive Model for Fiber Reinforced Thermoplastic Composites," *AIAA Journal*, Vol. 29, No. 3, 1991, pp. 457-463.

[6]Ha, S. K., Wang, Q., and Chang, F. K., "Modeling the Viscoplastic Behavior of Fiber-Reinforced Thermoplastic Matrix Composites at Elevated Temperatures," *Journal of Composite Materials*, Vol. 25, 1991, pp. 334-374.

[7]Saleeb, A. F., and Wilt, T. E., "Analysis of the Anisotropic Viscoplastic-Damage Response of Composite Laminates - Continuum Basis and Computational Algorithms," *International Journal for Numerical Methods in Engineering*, Vol. 36, No. 10, 1993, pp. 1629-1660.

[8]Dvorak, G. J., and Bahei-El-Din, Y. A., "Plasticity Analysis of Fibrous Composites," *Journal of Applied Mechanics*, Vol. 49, 1982, pp. 327-335.

[9]Chamis, C. C., and Hopkins, D. A., "Thermoviscoplastic Nonlinear Constitutive Relations for Structural Analysis of High Temperature Metal Matrix Composites," NASA TM 87291, 1985.

[10]Aboudi, J., "Micromechanical Analysis of Composites by the Method of Cells," *Applied Mechanics Reviews*, Vol. 42, No. 7, 1989, pp. 193-221.

[11]Hall, R. B., "Matrix-Dominated Thermoviscoplasticity in Fibrous Metal-Matrix Composite Materials," Ph. D. Dissertation, Rensselaer Polytechnic Institute, 1990.

[12]Kim, S. J., and Cho, J. Y., "Role of Matrix in Viscoplastic Behavior of Thermoplastic Composites at Elevated Temperature," *AIAA Journal*, Vol. 30, No. 10, 1992, pp. 2571-2573.

[13]Kim, S. J., and Shin, E. S., "A Thermoviscoplastic Theory for Composite Materials by Using a Matrix-Partitioned Unmixing-Mixing Scheme," *Journal of Composite Materials*, Vol 30, No. 15, 1996, pp. 1647-1669.

[14]Duhamel, J. M. C., "Memoire sur le Calcul des Actions Moleculaires Developpees par les Changements de Temperature Dans les Corps Solides," *Memoires Par Divers Savans*, Vol. 5, 1838, pp. 440-498.

[15]Neumann, F. E., *Vorlesungen uber die Theorie der Elasticitat der Festen Korper und des Lichtathers*, Leipzig, 1885, pp. 107-120.

[16]Oden, J. T., Bhandari, D. R., Yagawa, G., and Chung, T. J., "A New Approach to the Finite-Element Formulation and Solution of a Class of Problems in Coupled Thermoplasticity of Crystalline Solids," *Nuclear Engineering Design*, Vol. 24, 1973, pp. 420-430.

[17]Argyris, J. H., Vaz, L. E., and William, K. J., "Integrated Finite Element Analysis of Coupled Thermoviscoplastic Problems," *Journal of Thermal Stresses*, Vol. 4, 1981, pp. 121-153.

[18]Ghoneim, H., and Matsuoka, S., "Thermoviscoplasticity by Finite Element : Tensile and Compression Test," *International Journal of Solids and Structures*, Vol. 23, No. 8, 1987, pp. 1133-1143.

[19]Banas, A., Hsu, T. R., and Sun, N. S., "Coupled Thermoelastic-Plastic Stress Analysis of Solids by Finite-Element Method," *Journal of Thermal Stresses*, Vol. 10, 1987, pp. 319-344.

[20]Allen, D. H., "Thermomechanical Coupling in Inelastic Solids," *Applied Mechanics Reviews*, Vol. 44, No. 8, 1991, pp. 361-373.

[21]Odabas, O. R., and Sarigul-Klijn, N., "Thermomechanical Coupling Effects at High Flight Speeds," *AIAA Journal*, Vol. 32, No. 2, 1994, pp. 425-430.

[22]Shin, E. S., Yoon, K. J., and Kim, S. J., "Elasto-Viscoplastic Analysis of Composite Materials Considering Thermomechanical Coupling Effects," AIAA Paper 96-1578, April 1996.

[23]Miller, A. K. (Editor), *Unified Constitutive Equations for Creep and Plasticity*, Elsevier Applied Science Pub., 1987.

[24]Lubliner, J., *Plasticity Theory*, Macmillan Pub. Co., New York, 1990.

[25]Bodner, S. R., and Partom, Y., "Constitutive Equations for Elastic-Viscoplastic Strain- Hardening Materials," ASME *Journal of Applied Mechanics*, Vol. 42, No. 2, 1975, pp. 385-389.

[26]Chan, K. S., Lindholm, U. S., and Bodner, S. R., "Constitutive Modeling for Isotropic Materials (HOST) - Final Report," NASA CR 182132, 1988.

[27]Jones, R. M., *Mechanics of Composite Materials*, Scripta Book Co., Washington, D. C., 1975.

[28]Tsai, S. W., and Hahn, H. T., *Introduction to Composite Materials*, Technomic Pub. Co., Lancaster, 1980.

[29]Germain, P., Nguyen, Q. S., and Suquet, P., "Continuum Thermodynamics," *Journal of Applied Mechanics*, Vol. 50, 1983, pp. 1010-1020.

[30]Bathe, K. J., *Finite Element Procedures*, Prentice-Hall International Inc., 1996.

[31]Zienkiewicz, O. C., and Taylor, R. L., *The Finite Element Method*, 4th ed., Vol. 2, McGraw-Hill Book Company, 1991.

[32]Bass, J. M., and Oden, J. T., "Numerical Solution of the Evolution Equations of Damage and Rate-Dependent Plasticity," *International Journal of Engineering Science*, Vol. 26, No. 7, 1988, pp. 713-740